The TSI Radiometer Facility - absolute calibrations for total solar irradiance instruments

Greg Kopp, Karl Heuerman, Dave Harber, Ginger Drake
Univ. of Colorado / LASP, 1234 Innovation Dr., Boulder, CO 80303

ABSTRACT

The total solar irradiance (TSI) climate data record includes overlapping measurements from 10 spaceborne radiometers. The continuity of this climate data record is essential for detecting potential long-term solar fluctuations, as offsets between different instruments generally exceed the stated instrument uncertainties. The risk of loss of continuity in this nearly 30-year record drives the need for future instruments with <0.01% uncertainty on a absolute scale. No facility currently exists to calibrate a TSI instrument end-to-end for irradiance at solar power levels to these needed accuracy levels. The new TSI Radiometer Facility (TRF) is intended to provide such calibrations. Based on a cryogenic radiometer with a uniform input light source of solar irradiance power levels, the TRF allows direct comparisons between a TSI instrument and a reference cryogenic radiometer viewing the same light beam in a common vacuum system. We describe here the details of this facility designed to achieve 0.01% absolute accuracy.

Keywords: solar irradiance, TSI, Total Irradiance Monitor, Glory, SORCE

1. INTRODUCTION

Total solar irradiance (TSI) provides the primary energy driving the Earth's climate, and variations in the Sun's output are a natural climate forcing mechanism. Correlations between historical TSI and Earth temperature records give sensitivities to this solar forcing. These sensitivities rely on current TSI measurements from which historical estimates are derived via proxies which extend the record via extrapolation; thus accuracy of the current TSI measurements is critical in deriving solar forcing sensitivities needed to determine the natural causes of climate change.

The TSI record includes overlapping measurements from 10 spaceborne radiometers (see Fig. 1). The continuity of this climate data record has been essential, as offsets between different instruments generally exceed the stated instrument uncertainties; fortunately, a composite TSI record can be created because of temporal overlap between instruments (see Fig. 2). The risk of loss of continuity in this nearly 30-year record drives the need for future instruments with <0.01% uncertainty on a absolute scale. No facility currently exists to calibrate a TSI instrument end-to-end for irradiance at typical measured instrument power levels (30 to 80 mW of incident radiant power) to these needed accuracy levels, and the calibrations of the instruments in Fig. 1 are primarily at the component level prior to instrument assembly.

The NASA Glory mission is funding the creation of the TSI Radiometer Facility (TRF) to provide such end-to-end irradiance calibrations. The TRF, based on a cryogenic radiometer with a uniform input light source of solar irradiance power levels, allows direct comparisons between a TSI instrument and a reference cryogenic radiometer viewing the same light beam from within a common vacuum system. This facility will improve the calibration accuracy of future TSI instruments, establish a new ground-based radiometric irradiance standard, and provide a means of comparing existing ground-based TSI instruments against this standard under flight-like operating conditions.

This paper describes the details of the TRF. Section 2 describes the design considerations of the TRF, and §3 the hardware implementation of this new facility being built in a dedicated optics lab at the Laboratory for Atmospheric and Space Physics at the University of Colorado in Boulder.

Earth Observing Systems XII, edited by James J. Butler, Jack Xiong,
Proc. of SPIE Vol. 6677, 667709, (2007) · 0277-786X/07/$18 · doi: 10.1117/12.734553

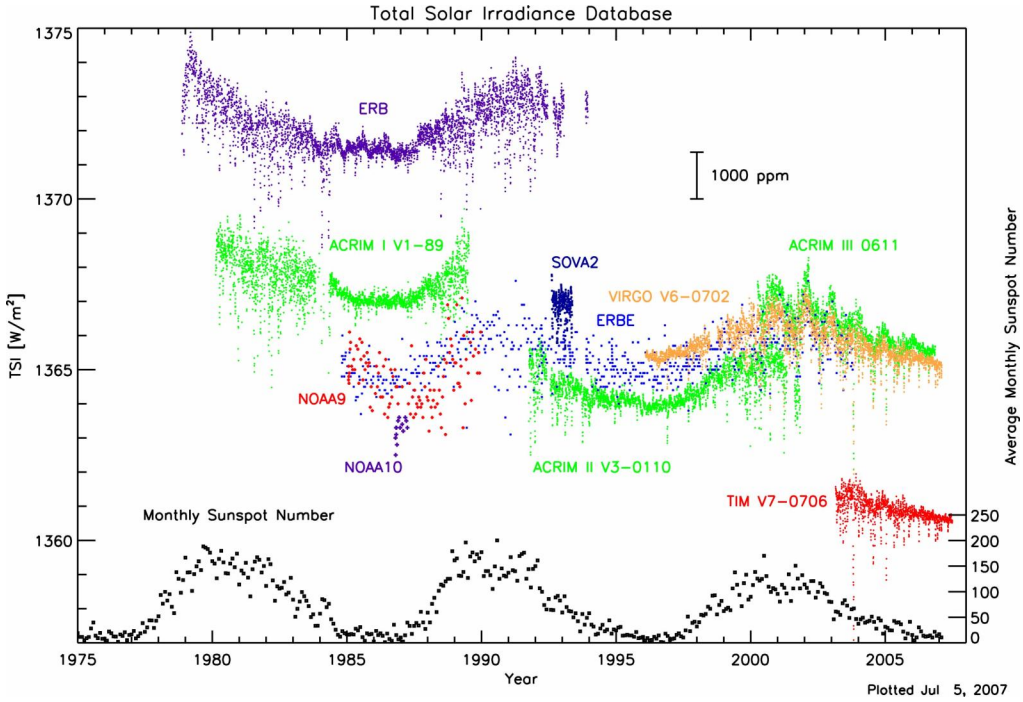

Fig. 1. The TSI climate data record is nearly 30 years long and includes measurements from 10 spaceborne solar radiometers. Offsets between instruments are due to unresolved instrument calibrations.

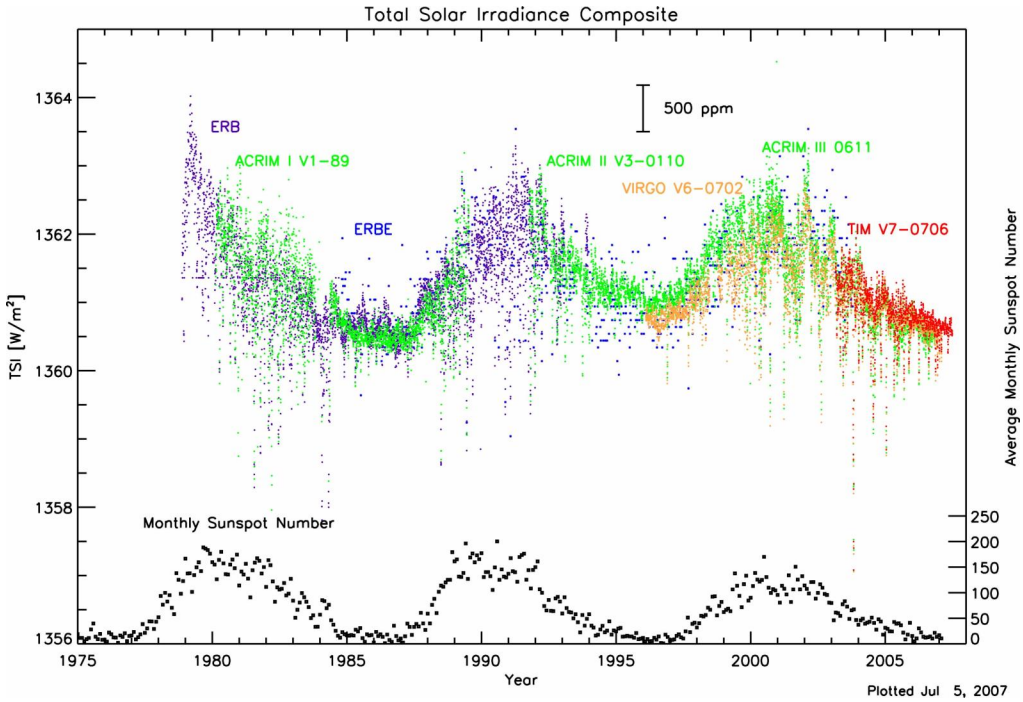

Fig. 2. Temporal overlap between instruments contributing to the TSI data record allows the creation of a composite TSI record by normalization to a chosen absolute value. This composite shows the nearly sinusoidal solar variability over the 11-year solar cycle (indicated by the sunspot number at the bottom of the plot) as well as larger short-term solar fluctuations due to the creation of or the passage across the Sun's surface of solar active regions.

2. TRF DESIGN CONSIDERATIONS

2.1 TRF Requirements

Previous ground-based comparisons of TSI instruments, such as those performed at the World Radiation Center in Davos, Switzerland or at NASA JPL's Table Mountain in California, have inherent limitations affecting absolute accuracy – this is not unexpected since achieving absolute accuracy was not the original intent with either of these facilities. Davos's World Radiation Reference (WRR) is a >30-year comparison of measurements from several ground-based TSI instruments. The average of a small set of these instruments gives a measure against which other radiometers can be compared on a relative scale. While this allows for comparisons of similarly-designed instruments and a link to an established time record, the link to absolute, or SI, units has uncertainties of nearly 0.3% (1) with possible limitations caused by observing the Sun through the Earth's atmosphere and operating the TSI instruments in air. JPL's Table Mountain facility similarly observes through the Earth's atmosphere, but operates the TSI instruments in a common vacuum tank and applies corrections for the transmission losses of the vacuum window in front of each instrument. Good at indicating *relative* differences between instruments, this facility is not linked to SI units to determine which instruments under test have the best absolute accuracy.

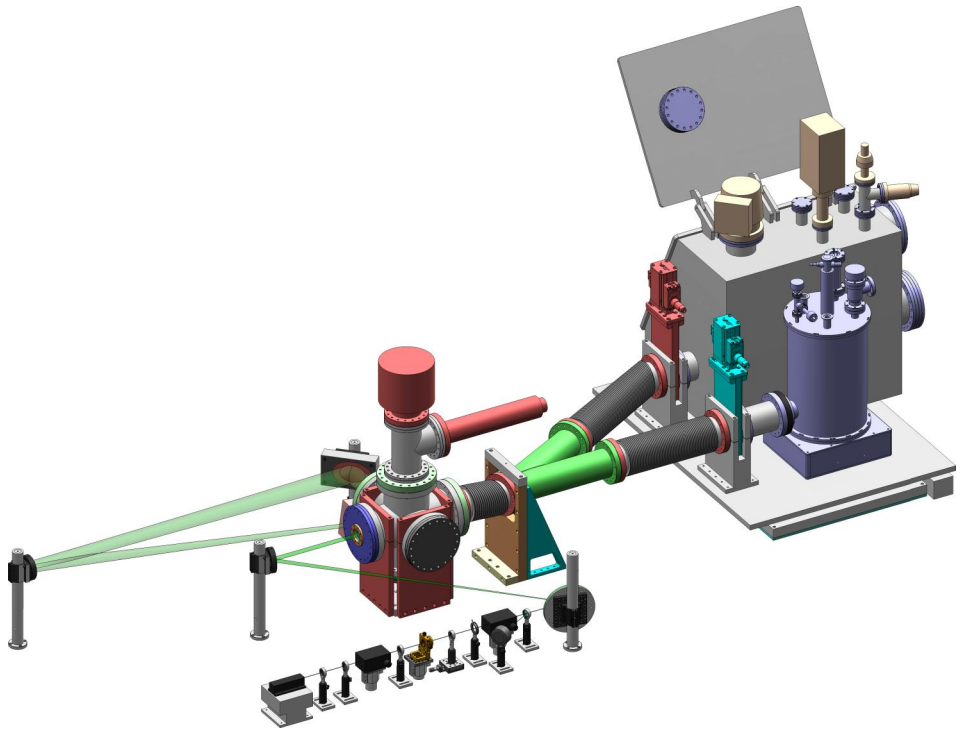

Fig. 3. The TSI Radiometer Facility allows direct comparison of the irradiance measurements of a uniform input light beam (foreground, incident to the vacuum system from the left) between a cryogenic radiometer (cylindrical dewar shown on right) and a TSI instrument contained within the adjacent vacuum tank (right, rear). A translation stage holding both the TSI instrument and the cryogenic radiometer translates either into precisely the same portion of the incident radiant beam. Flexible vacuum bellows in the Y-shaped arms contain the entering beam in a common vacuum system so that the beam enters through a single vacuum window and remains stationary. An imaging camera system (rear) monitors radiometer aperture position to assure identical placement of either radiometer in the light beam.

The TRF is intended to compare a TSI radiometric instrument to a reference standard cryogenic radiometer having NIST traceability of its absolute scale. Both the TSI instrument and the cryogenic radiometer operate in vacuum, eliminating uncertainties caused by operating thermal radiometers with convective and conductive air losses and the resulting non-equivalence issues from these difficult to characterize thermal paths. Since both the TSI instrument and the cryogenic radiometer are in a common vacuum system and translated into the incoming radiant beam, both radiometers sample the same portion of the beam through the same portion of the entrance vacuum window, eliminating the sizeable corrections needed when transmitting through different window locations. The TRF provides the same uniform, collimated, solar-power level laboratory light source to both the TSI instrument and the reference cryogenic radiometer, so that

uncertainties in radiometer fields of view coupled with background circumsolar scatter corrections caused by observing through the Earth's atmosphere are nonexistent.

The basic concept of the TRF is that either the TSI instrument under test or the cryogenic radiometer can be translated to observe an identical portion of a stationary and stable incident radiant light source providing solar levels of power. A common vacuum system into which the stationary radiant beam is transmitted eliminates thermal complications of operating a radiometer in air. An overview of the TRF is shown in Fig. 3 and the implementation details are presented in §3. The high-level TRF requirements on the cryogenic radiometer are given in Table 1.

Table 1. TRF Cryogenic Radiometer Requirements

Parameter	Requirement	Units
Nominal Measured Irradiance Level	1360	W/m^2
Accuracy	67.2	ppm
	0.004588	mW
Cryo Aperture Area	0.50204956	cm^2
Aperture Radius	*3.9976*	mm
Aperture Diameter	*7.9952*	mm
Nominal Measured Power Level	*68.3*	mW
Noise, k=1	2	ppm
	0.000137	mW
TSI Instr Aperture Area	0.505886	cm^2
TSI Instr Aperture Radius	*4.0128*	mm
Cryo/TIM Aperture Agreement	*7584*	ppm
	0.0152	mm
Measurement Time	10	min
Electrical Power Linearity	10	ppm
	0.000683	mW
Spectral Range, nominal	532	nm
Spectral Range, operational	400-1550	nm
Minimum Continuous Operational Time	13	hrs

2.2 Inherent Radiometer Uncertainties

The estimated uncertainties for the cryogenic radiometer are similar to those for very accurate TSI instruments, such as those given by Kopp *et al.* (2) for the SORCE Total Irradiance Monitor (TIM). Cryogenic radiometers benefit from superconducting electrical leads, faster radiometer thermal response and thus reduced effects of non-equivalence, and reduced thermal background. Additionally, being a lab-based reference that will never be exposed to unfiltered sunlight above the Earth's atmosphere, the cryogenic reference radiometer does not require a space-quality robust absorptive coating on the internal light-absorbing radiometer cavity, so it can use a more efficient absorbing material to reduce reflections and similarly reduce uncertainties. Estimates of the contributing uncertainties to the cryogenic radiometer's accuracy for measuring irradiances at solar power levels are given in Table 2. The cryogenic radiometer for the TRF was designed to have a similar optical layout – including the cavity entrance area, aperture area and design, and cavity-to-aperture distance – as the TIM described by Kopp and Lawrence (3), so that similar optical and diffractive corrections and uncertainties apply to both.

The intent with the TRF is to compare irradiance measurements of a TSI instrument against this cryogenic radiometer, and that comparison will introduce additional uncertainties from those given in Table 2. Such effects include: the intrinsic accuracy of each radiometer itself; the beam intensity stability between measurements with each radiometer; differences in thermal background and scattered light from each radiometer's entrance onto surrounding baffles; aperture area differences causing different beam sampling; positioning of each radiometer to sample the same portion of the incident beam; and pointing or alignment of each radiometer. Estimates of these effects are summarized in Table 3 and detailed in following sections; these limit expected comparison differences to values much higher than the intrinsic accuracy of the TRF's cryogenic radiometer alone.

Table 2. Estimated Cryogenic Radiometer Uncertainties

Correction	Value [ppm]	σ [ppm]
Aperture	1,000,000	31
Diffraction	452	46
Cone Reflectance	5	5
Non-Equivalence, ZH/ZR - 1	0	7
Servo Gain	5,000	5
Standard Volt + DAC	1,000,000	10
Linearity	1,000,000	10
Standard Ohm + Leads	1,000,000	10
Dark Signal	2,500	10
Scattered Light	200	30
Pointing (Aperture Alignment)		1
Measurement Repeatability (Noise)		1.0
Total RSS		**67.2**

Table 3. TRF Comparison Uncertainties

Parameter	σ [ppm]
Cryogenic Radiometer Uncertainty	67
TSI Instrument Uncertainty	100
Beam Stability Knowledge	100
Thermal Background	104
Scattered Light Differences	50
Aperture Area Differences	10
Stage Positioning	1
Pointing	54
Total RSS	**202**

2.3 Instruments Operate in Common Vacuum

The cryogenic radiometer must be operated in vacuum to achieve its operating temperature. TSI instruments are designed to work in vacuum so that the thermal and radiative paths affecting the radiometer's measurements are not complicated by additional convective or conductive paths due to air. To achieve the accuracy levels intended with the TRF, both instruments must operate in vacuum.

So that both radiometers also sample the incident radiant beam identically, no additional optics or windows can alter the beam when translating the radiometers into the beam. Thus the two radiometers are contained in a common vacuum system with a single optical entrance window for the light source. This entrance window and incident beam are stationary, so transmissive losses are identical for each radiometer and do not contribute to comparison differences.

2.4 Beam Intensity and Stability

The incident beam must supply radiant power equivalent to the Sun and must have temporal stability such that intensity fluctuations on the time scales of the comparisons between radiometers do not limit the uncertainties. To achieve radiant power levels comparable to the TSI instruments having the largest entrance apertures, roughly 70 mW of radiant power is needed to uniformly cover an 8-mm diameter area. With 15-minute measurement time scales for the TSI instrument or the cryogenic radiometer, beam stabilities over these time scales should be limited to approximately 0.01%. Monitoring beam intensity with a separate photodiode may help achieve knowledge of beam intensity to this level, but introduces additional potential errors sources.

2.5 Thermal Background

Since both the TSI instrument and the cryogenic radiometer are fundamentally bolometric radiometers, they are both sensitive to visible and infrared radiation, and thus can be affected by their internal and external thermal environments. For external sources to have little effect on comparisons, they should be small and/or should be nearly identical between radiometers. Making them small means thermally cooling all viewable external sources to nearly cryogenic temperatures, which is not practical with the extensive vacuum system in the TRF. Making them nearly identical means making the view factors of the radiometers similar. Thus the cryogenic radiometer has been designed to have similar aperture area and cavity entrance area separated by the same longitudinal distance as in the TIM instrument, which will be the first used in the TRF prior to its launch on NASA's upcoming Glory mission.

By chopping the incident beam and applying phase sensitive detection methods, thermal background sources are greatly reduced. The chopping of the light beam occurs as far upstream of the instrument as possible so that only the light is modulated, and each radiometer individually subtracts out its thermal background contribution.

On-orbit data from a TSI instrument suggests that the instrument's internal thermal signals can be corrected to roughly 0.001%; however the external thermal contributions in a lab are much greater than they are on-orbit, and unaccounted for changes during a measurement are estimated at nearly 0.005 mW, or a 0.007% uncertainty. Since the comparison involves similar contributions from both the TSI instrument and the cryogenic radiometer, the thermal background uncertainty estimate in Table 3 is likely conservatively overstated.

2.6 Scattered Light

Some sizeable portion of the incident light will reflect or scatter off the front surfaces on each radiometer. The much smaller portion of this light that reflects from vacuum system components and is then scattered back through the radiometer's aperture can be measured and will lead to erroneously high irradiance measurements. This scattered light is reduced by baffling and light control from the front of the radiometers to reduce reflection paths back toward the radiometers. Identical specular black baffles in front each radiometer control these reflections to send them further from the radiometer and reduce backscatter. Having nearly identical baffle arrangements in front of each radiometer will also make such reflections common to both, reducing systematic differences between the measurements with each radiometer. Scattered light is further reduced by internal radiometer baffles that reject off-axis light entering the aperture.

2.7 Beam Profile

In the TRF, the two radiometers are translated into the stationary light beam. An alternate approach of steering the beam into the radiometers would introduce variations in the beam intensity or beam profile and cause differences in the measurements. Leaving the beam stationary reduces these differences but relies on good beam stability and a uniform beam profile with accurate aperture placement when translating the radiometers.

To accurately compare measurements of the incident light beam with the TSI instrument and the cryogenic radiometer, they must each collect the same amount of radiant power through their entrance aperture. Placement of the radiometer apertures so that they sample the same portion of the incident beam mitigates effects from possible non-uniformities in the beam. Two causes of differences in radiometer measurements due to sampling different portions of a potentially non-uniform beam profile are different radiometer aperture areas, and different positioning of the apertures in the beam. The more uniform the beam, particularly at the edges of the apertures, the lower the uncertainties caused by both aperture size and positioning.

Consider a reasonably uniform beam of some width r_b much larger than the aperture radius r_a so that it has relatively small variations across the portion collected by the aperture. Allow some positioning offset u between the center of the beam and the aperture center. Fig. 4 shows an example of this general beam.

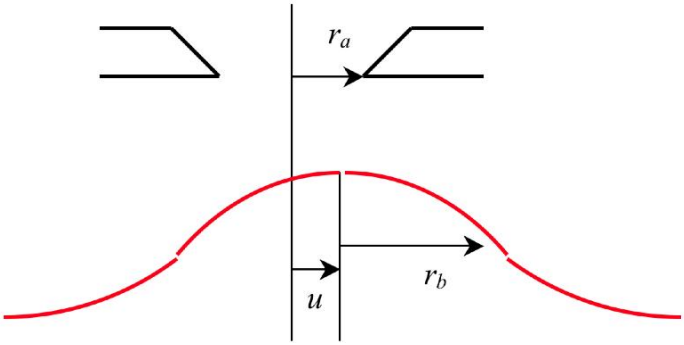

Fig. 4. A beam of profile $I(r)$ with large effective width $r_b \gg r_a$ is incident on a circular aperture or radius r_a but offset from the aperture center a distance u, creating asymmetry in the sampled portion of the beam.

2.7.1 Different Sized Apertures Centered on Symmetric Beam

For apertures centered on a symmetric beam with irradiance $I(r)$, the sampled beam may have a different value $I(r_a)$ at the aperture edge. Measuring this beam with slightly different sized apertures will affect the comparison, so *it is important that both radiometers have similar sized apertures*. Apertures differing in radius by a small amount Δr but centered at the same position r=0 will only differ because of the light collected near the outer edge. For example, the measured radiant power P_2 for a slightly larger radius aperture $r_2=r_a+\Delta r$ (with $\Delta r>0$) will be slightly lower for a monotonically decreasing beam profile since the extra collected light near the aperture edge has slightly lower intensity. More generally, let the irradiance measured by one radiometer be

$$I_1 = \frac{P_1}{\pi r_a^2} = \frac{1}{\pi r_a^2}\int_0^{r_a} 2\pi r \cdot I(r)\,dr. \qquad (1)$$

The other radiometer measures irradiance from a slightly different portion of the beam $r_a+\Delta r$, so collects light of possibly different irradiance $I(r_a)$ that could also be changing with radius by slope $\partial I/\partial r$. This gradient is 2nd order in Δr,

$$I_2 = \frac{P_2}{\pi r_2^2} = \frac{P_1 + \int_{r_a}^{r_a+\Delta r} 2\pi r \cdot I(r) dr}{\pi\left(r_a + \Delta r\right)^2}$$

$$\approx \frac{1}{\pi r_a}\left(1 - \frac{2\Delta r}{r_a} + \frac{3\Delta r^2}{r_a^2}\right)\left[P_1 + 2\pi r_a \Delta r I(r_a) + \pi \Delta r^2 I(r_a) + \pi r_a \Delta r^2 \left.\frac{\partial I}{\partial r}\right|_{r_a}\right]$$

(apertures centered on beam)
$$\boxed{I_2 \approx I_1 - \frac{2\Delta r}{r_a}\left[I_1 - I(r_a)\right] + \frac{3\Delta r^2}{r_a^2}\left[I_1 - I(r_a)\right] + \frac{\Delta r^2}{r_a}\left.\frac{\partial I}{\partial r}\right|_{r_a}} \quad (2)$$

The irradiance differences due to aperture radii differences can be due to both a beam slope correction and a change in the beam from center-to-edge. The terms $[I_1\text{-}I(r_a)]$ account for the differences between the irradiance averaged over the aperture and that right at the aperture edge. The derivative term accounts for high spatial frequency changes right at the aperture edge. Thus the differences when comparing radiometer measurements with two slightly different-sized apertures centered on a symmetric beam *is very sensitive to the beam profile right at the aperture edge*.

Note for a uniform beam that $I_2=I_1$ in Eqn. 2. Similarly, for identical apertures ($\Delta r=0$), $I_2=I_1$ regardless of beam profile. More generally, for a beam with intensity decreasing with radius, I_2 is slightly lower than I_1. For smoothly-varying beams such as Gaussians, the center-to-edge effects are larger, but for high spatial frequency beam variations the slope correction can be significant. If the beam profile is known, these effects can be corrected, so the uncertainty in measurement is due to the uncertainty in the beam profile knowledge.

Since the irradiance differences are the result of aperture radii differences, the cryogenic radiometer aperture size should match that of the TSI instrument under test to reduce the effects from potentially non-uniform beam profile. For the TRF, the aperture for the cryogenic radiometer came from the same lot of apertures procured from and calibrated at NIST/Gaithersburg for the Glory/TIM TSI instrument, allowing good comparisons between these two radiometers.

2.7.2 Aperture Positioning

There will be a first-order effect from not positioning the two radiometer apertures in the same location of the radiant beam. If identical radiometer apertures are misplaced some distance and direction $\vec{u}$, the difference in irradiance measurements with the two radiometers caused purely by this positioning error is

$$I_2 - I_1 = \frac{1}{\pi r_a^2}\int_0^{r_a} 2\pi r \cdot I(\vec{r} + \vec{u}) dr - \frac{1}{\pi r_a^2}\int_0^{r_a} 2\pi r \cdot I(r) dr. \quad (3)$$

As the beam profile can vary in two dimensions and may not be symmetric about the center, and the integral over the apertures depends on the displacement $\vec{u}$ and the normal to the aperture edge, these integrals can be complex analytically. The important point from Eqn. 3 is that for small misplacements $\vec{u}$ the sensitivity to aperture position depends mostly on the gradient of the beam profile near the aperture edge. The beam profile, particularly at the edges of the apertures, determines the comparison uncertainties attributable to aperture positioning and drives requirements on the translation stage accuracy. In §3.3 we determine the sensitivity to aperture placement for a sample TRF beam.

2.8 Pointing

Each instrument needs to be placed with its aperture perpendicular to the incident beam. Non-normal incidence can have complicated effects, including changes in the illuminated portion of the radiometer cavities and radiative to electrical heating non-equivalence. Aside from those more subtle effects, the aperture area changes by the cosine of the angle of the incident light from normal. Differences between the angular alignments of the two radiometers relative to the illuminating beam will thus cause a pointing uncertainty.

3. IMPLEMENTATION

The TRF implementation utilizes a monochromatic light source entering a vacuum system common to both the cryogenic and the TSI radiometers. Either radiometer can be placed in the incident beam by translation perpendicular to the beam such that the aperture from each is located in almost exactly the same portion of the beam for the reasons discussed in §2.7. One radiometer acquires a measurement of the beam for some time, then the radiometers are switched and the other acquires a measurement. The light source is monitored continually to track intensity stability.

3.1 Radiometers Measure Irradiance

The cryogenic radiometer and the TSI instruments operate on similar principals. The TIM TSI instrument intended for test on the TRF prior to flight on the Glory mission was designed and built at the University of Colorado's Laboratory for Atmospheric and Space Physics. The TRF cryogenic radiometer, able to measure radiant power levels exceeding the typical TSI levels, is being manufactured by L-1 Standards and Technology, Inc. This is a liquid-helium cooled radiometer to reduce electrical heating lead resistances and thermal background. Both radiometers measure irradiance, generally expressed in units of W/m^2.

The absorptive cavities of the radiometers absorb and spectrally integrate incident radiant light yielding a measure of the total radiant power. The TIM radiometer cavities are made of silver with an etched nickel phosphorous interior that absorbs ~99.98% of the incoming solar broadband radiation. The cryogenic radiometer for the TRF utilizes a copper cavity having very high thermal conductance at operating temperatures. A servo system applies electrical power to maintain constant cavity temperature, and the modulation of this electrical heater power as incident light is modulated is a direct measure of the absorbed radiant power.

Precision 8-mm diameter apertures define the area over which the incident radiation is collected. The apertures for both the TIM TSI instrument and the cryogenic radiometer are diamond turned from nickel plated Al 6061-T6 and have a knife edge radius approaching 1 µm. The geometric areas of the apertures were measured at NIST in the Optical Technology Division and have a 1-sigma uncertainty of approximately 0.0025% using the measurement technique described by Fowler and Litoria (4). A thermistor is mounted on each aperture base plate so the area can be corrected for temperature. The cryogenic radiometer aperture is not cooled, so such corrections are small and introduce little additional uncertainty. The aperture used in the TRF cryogenic radiometer is from the same lot as the Glory/TIM flight apertures. Having such nearly identical apertures reduces sensitivities to potential beam profile effects described in §2.7.

3.2 Vacuum System

Using flexible bellows and rotating about a single pivot point, the vacuum system is designed to position either the cryogenic or TSI radiometer into the light beam path. An external drawing of the TRF is shown in Fig. 3. Positioned roughly in the center of the optical table is the light beam entrance to the vacuum system. This entrance is a single super-polished BK7 window with 532 nm V-coatings on both surfaces. Both radiometers sit on a 48-cm range motorized translation stage with 2–µm repeatability. This precision stage can center either radiometer into nearly the same position in the incoming radiant beam. When the stage moves, the vacuum manifold pivots about a single point where the two arms of the Y-bellows meet. Flexible bellows accommodate changes in vacuum arm path length and mounting angles during movement. Two gate valves separate the radiometers from the rest of the vacuum manifold creating three vacuum regions, each having a separate pumping system capable of achieving high vacuum ($<10^{-7}$ Torr) and allowing for independent pumpdown of the cryogenic radiometer, the TSI instrument and surrounding vacuum tank, and the Y-bellows portion of the vacuum system. Aside from the entrance and exit windows, the vacuum system is opaque and shields stray laboratory light from the radiometers. Internal baffles near the radiometer apertures reduce scattered light effects from the incident beam. Fig. 5 shows a cutaway of the TRF setup with the TIM TSI instrument in the incident beam; Fig. 6 shows the cryogenic radiometer in the beam.

Although some TSI instruments, such as the TIM, have self-containing vacuum cases to provide contamination control during ground phases of spacecraft build-up and integration, the TRF includes a vacuum tank surrounding the entire TSI instrument to accommodate those instruments that do not have self-containing vacuum tanks.

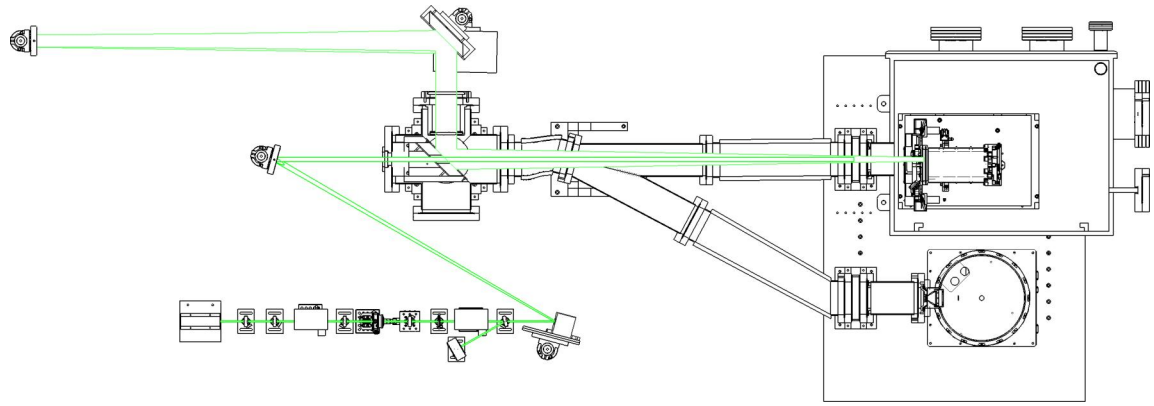

Fig. 5. With the TSI instrument illuminated, the translation stage is positioned so that the incident beam travels along one arm of the vacuum bellows onto the center of the TSI aperture. The vacuum bellows to the TSI instrument is compressed, while that to the cryogenic radiometer is extended.

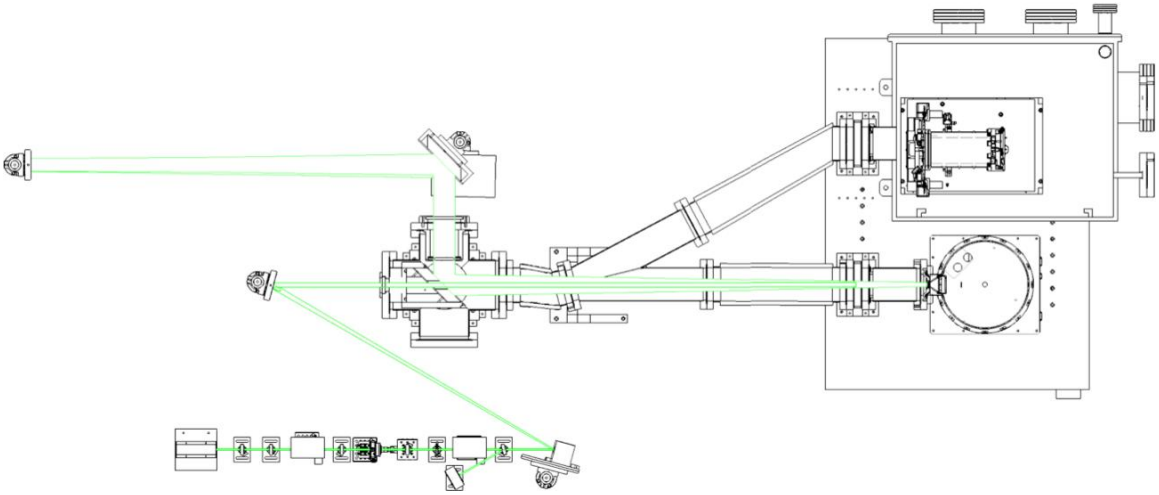

Fig. 6. To illuminate the cryogenic radiometer, the translation stage moves so as to pivot the vacuum arms about the mount holding the rigid Y, allowing the incident beam to travel directly to the cryogenic radiometer's aperture.

3.3 Incident Beam Is Stable and Uniform

For accurate comparison between the radiometers the light source must be stable in intensity and spatial distribution for durations particularly on the order of comparison times (~30 minutes for a single comparison between the TSI instrument and the cryogenic radiometer).

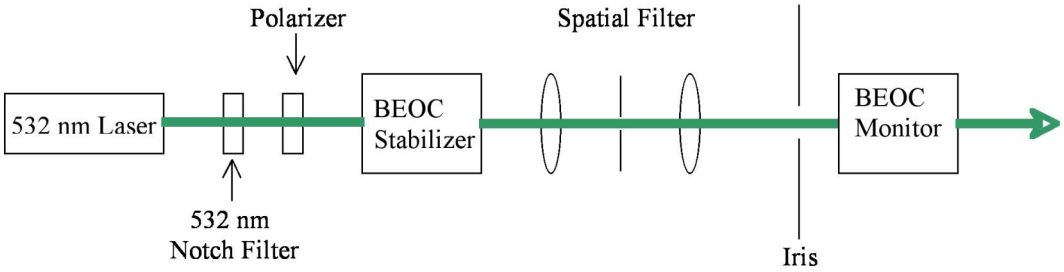

Fig. 7. Beam is intensity stabilized prior to the fast steering mirror.

The beam is created by a 500 mW diode pumped CrystaLaser 532 nm laser internally stable to 0.5%. A Brockton Electro-Optics Corporation LPC closed-loop laser stabilizer is used to further stabilize the laser intensity to ~0.01%. The

optics for creating and intensity stabilizing the beam are shown in Fig. 7. A photodiode monitors beam intensity. Since the silicon photodiode sensitivity is linearly proportional to laser frequency while the radiometers are not, this beam monitor is merely a diagnostic of laser stability. A typical plot of intensity over time is shown in Fig. 8, and demonstrates variations over typical comparison measurement times of <0.01% . Long-term variations are likely due to residual temperature fluctuations in the thermal isolation box surrounding the optics; the short-term (100-s) variations are due to chopping the beam to measure thermal backgrounds, and do not affect radiometer measurements.

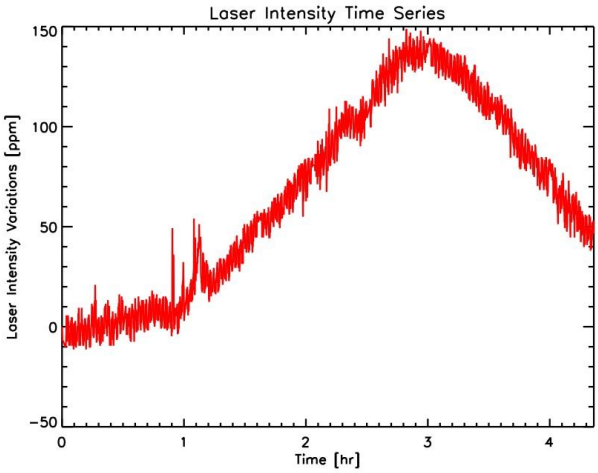

Fig. 8. Time series of laser intensity shows low-frequency variations at the 0.015% level over a few hours. Variations on time scales of the ~30 min radiometer inter-comparison period are much lower.

As detailed in §2.7, comparisons between the cryogenic radiometer and the TSI instrument are most sensitive to beam profile near the aperture edges. Methods of providing a spatially uniform beam for the TRF have different advantages. A broad Gaussian beam can be very uniform over the aperture area; however, to have sufficiently low gradients near the aperture edges and to provide typical solar power levels, this beam must exceed 10 cm in width and requires over 5 W of power, most of which is wasted in the wings of the beam where it may cause scatter problems when reflected off the instrument. A refractive beam shaper, such as that marketed by Newport (GBS-AR14), improves beam uniformity across a small central beam region, keeping the beam spatially confined and reducing power requirements; but such beam shapers are sensitive to figure errors of the optics. These figure errors create small spatial scale intensity fluctuations on the order of several percent that worsen as the beam propagates (5). Such high frequency spatial variations could affect the beam profile near the aperture edges, which is where the sensitivity to aperture positioning and aperture area described in §2.7 are greatest.

The TRF instead uses an innovative spiral beam scanning approach. An intensity stabilized laser beam is scanned uniformly across the radiometer aperture area in a time much shorter than the thermal response time of the radiometer. Since this beam is mostly collected by the aperture and therefore has low light losses, the beam power levels are very modest at only the ~70 mW of power typical of the TSI instrument under test.

After considering different scanning methods including quickly rotating polygonal mirrors, a more efficient spiral beam scanning method driven by a 2-axis fast steering mirror was selected and tested for use in the TRF. This spiral beam has advantages in efficiency, low light loss and scatter, and required power level. The input beam is scanned in a spiral pattern to cover the aperture area uniformly, spending nearly equal amounts of time in each portion of the aperture by maintaining constant linear beam velocity. The 0.4 mm spacing between successive spirals in the pattern is smaller than the ~2 mm laser beam diameter for good spatial uniformity. A concave mirror after the fast steering mirror collimates the spiral beam. The entire spiral pattern filling the aperture area is scanned at 10 Hz, which is faster than the radiometer response times so that they effectively integrate the incident beam energy over several spiral patterns. Fig. 9 shows a plot of the spiral pattern of the beam center and the 2-axis movement over time. Note that the highest response frequencies needed from the 2-axis fast steering mirror are near the center of the spiral pattern, where mirror displacements are the lowest and the analysis in §2.7 shows low sensitivity to beam non-uniformities that could potentially be caused by non-linearities in mirror response.

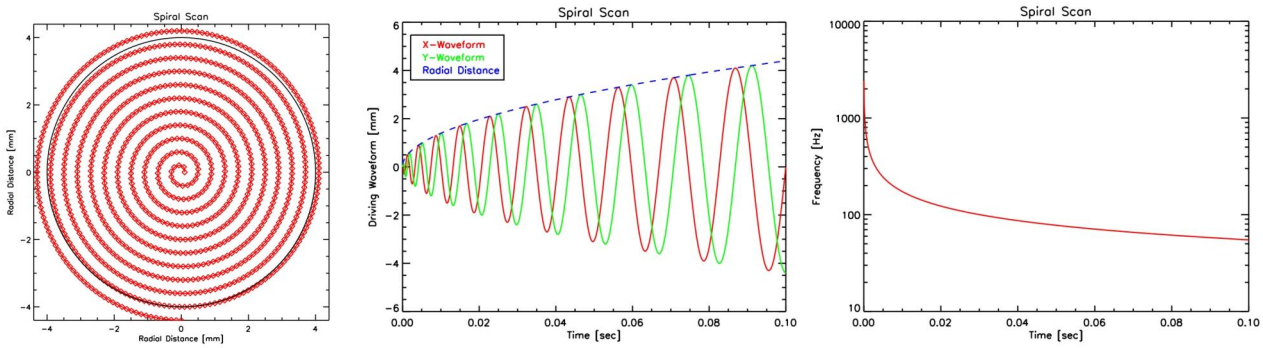

Fig. 9. The spiral beam scanning method (left and middle) concentrates possible non-linearities at high frequency responses (right) of the fast steering mirror at the center of the beam where the sensitivity to intensity variations is small, keeping the beam profile at the aperture edges uniform.

A demonstration of this 2-axis spiral beam scanning method shows good spatial uniformity and sufficiently fast mirror response. Fig. 10 shows a CCD image of the uniform illumination beam created by the spiral scanning technique of a >2 mm laser beam. Cuts across this beam show good uniformity. The non-uniformities near beam center are due to fast steering mirror response non-linearities at the high frequencies needed to create this scanning beam; these spatial intensity non-uniformities are isolated to a portion of the beam where their effects are largely irrelevant. The TRF will use a smaller and faster steering mirror than that in this proof-of-concept, further improving beam uniformity.

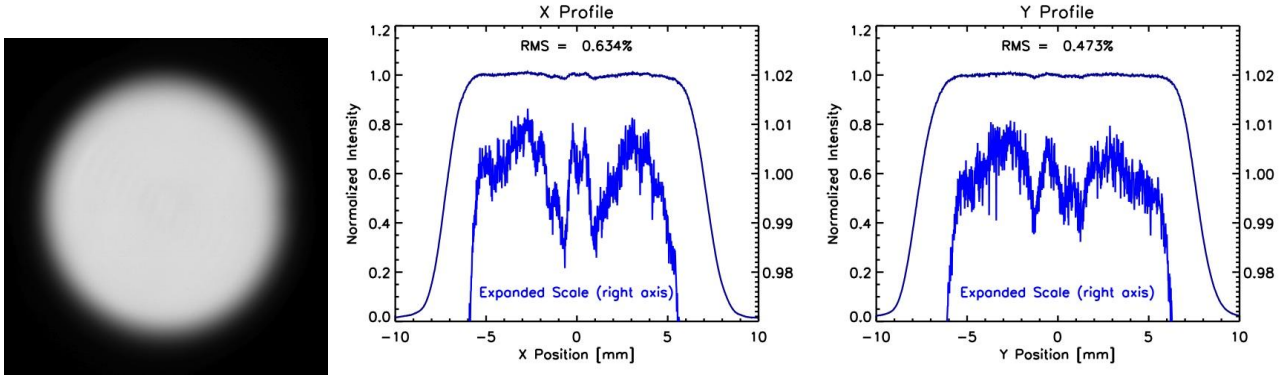

Fig. 10. CCD image of the spiral beam (left) shows good uniformity across diameters (right) with non-linearities mainly at the beam center.

From beam intensity images, sensitivity to aperture area and aperture positioning are computed and used to determine required positioning tolerances. Fig. 11 shows the derived sensitivities from the beam profile in Fig. 10, and is used to derive the uncertainty estimates for the TRF comparisons in Table 3 and the positioning and area matching requirements in Table 1.

3.4 Aperture Position Monitor

From the beam profile data in §3.3, relative aperture positioning accuracies of 10 µm are sufficient for comparisons between the TSI instrument under test and the cryogenic radiometer. An aperture imaging camera system provides confirmation of each radiometer's aperture position, which is controlled by both horizontal and vertical translation stages. The radiometers are mounted on a horizontal stage with a repeatability of 2 µm, and the TSI instrument is additionally mounted on a vertical stage having <3 µm step size to provide relative adjustment of its aperture to that of the cryogenic radiometer's. Monitoring of the actual aperture position is done with a Pixel View camera having a 1024 x1024 CCD array with 25 µm pixels and 1-to-1 re-imaging of the radiometer apertures via a 1-m focal length lens mounted within the vacuum system. Fitting the aperture image to a circle allows sub-pixel positioning resolution; aperture positioning requirements only rely on resolution at the modest 2/5 pixel level. Illumination of the apertures is provided by the reflection off the aperture from the incident beam.

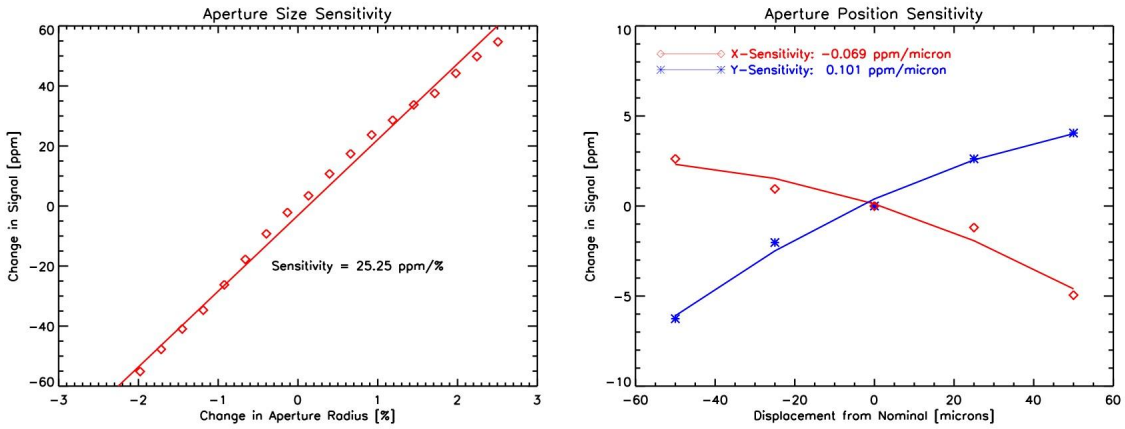

Fig. 11. Sensitivities of the spiral beam to aperture area differences (left) and position (right) are low due to good uniformity at the aperture edges.

4. SUMMARY

The TSI Radiometer Facility will provide end-to-end irradiance calibrations of TSI instruments. This will be the first facility to compare a TSI instrument directly against a cryogenic radiometer with each sampling the same input radiant beam. The facility will work in irradiance mode rather than merely measuring optical power. Both the TSI instrument under test and the cryogenic radiometer are operated in vacuum, as designed, and the common vacuum system allows both to measure the same input light beam with no additional optics.

This facility will improve the calibration accuracy of future TSI instruments, establish a new ground-based radiometric irradiance standard, and provide a means of comparing existing ground-based TSI instruments against this absolute standard under flight-like operating conditions.

REFERENCES

1. Willson, R., "Active cavity radiometer type V," *Applied Optics*, 18, 2, Jan. 1979, pp. 179-188.
2. Kopp, G., Heuerman, K., and Lawrence, G., "The Total Irradiance Monitor (TIM): Instrument Calibration," *Solar Physics*, 230, 1, Aug. 2005, pp. 111-127.
3. Kopp, G. and Lawrence, G., "The Total Irradiance Monitor (TIM): Instrument Design," *Solar Physics*, 230, 1, Aug. 2005, pp. 91-109.
4. Fowler, J. and Litorja, M., "Geometric Area Measurements of Circular Apertures for Radiometry at NIST," *Metrologia*, 40, 2003, pp. S9-S12.
5. Hoffnagle, J. and Jefferson, M., "Beam shaping with a plano-aspheric lens pair," *Optical Engineering*, 42, 2003, pp. 3090-3099.

ACKNOWLEDGEMENTS

We are grateful to the NASA Glory mission (NNG04HZ05C) for providing funding for this new facility.